SciMedCentral

JSM Chemistry

Short Communication

Studying Structural Properties of ZnO: Pb_3O_4 Particles with Different Concentration

Ahmad Khoudro, Sallama Abo Alshamlat, Heleen Massoud*

Department of physics, Faculty of science, Tishreen University, Syria

*Corresponding author
Heleen Massoud, Department of physics, Faculty of science, Tishreen University, Syria; Email: heleenmassoud@gmail.com

Submitted: 03 January 2023

Accepted: 18 January 2023

Published: 20 January 2023

ISSN: 2333-6633

Copyright

© 2023 Khoudro A, et al.

OPEN ACCESS

Keywords

- Powder
- Iron and Antimony doped Tin Oxide
- Solid state reaction
- Structural properties

Abstract

Zno, Pb_3O_4 doped tin oxide transparent conducting powder were prepared by solid-state reaction method. Structural properties of the samples were investigated as a function of various Zno, Pb_3O_4 doping levels (x=0.0- 0.2- 0.5- 0.8). The results of x-ray diffraction have shown that the samples are polycrystalline structure in tetragonal phase with preferential orientations along the (110) for all samples. The relative intensities, distance between crystalline planes (d), crystallite size (D), dislocation density (δ) and lattice parameters (a), (c).

INTRODUCTION

One of the most important semiconductors are the so-called transparent conduction oxides (TCO), which are compound semiconductors composed of metal combined with oxygen, that is, they are oxide conductors as (SnO_2, ZnO_2, In_2O_3), and despite their large energy gap, the conduction band is full of free electrons due to the oxygen vacancies resulting from non-stoichiometry [1]. Translucent conductive oxides are characterized by a wide energy band change from 3eV to 5eV. This wide depends on several factors including: the type of solution compounds, deposition method and experimental conditions for sedimentation.

One of these oxides is zinc oxide, which is a white, solid, pure compound, yellows on heating due to retinal abnormalities, it is non-toxic substance that does not dissolve in water or alcohol but rather dissolve in acetic acid, mineral acids, ammonia, ammonium carbonate and alkaline hydroxides. In preparing zinc oxide chemically laboratories depend on burning zinc in the air or by thermal smashing of its carbonates or nitrates, (Table 1) shows some of its properties [2].

Zinc oxide crystallizes in a hexagonal lattice, where the oxygen atoms occupy the hexagonal lattice sites, while the zinc atoms occupy half of the quaternary sites.

The average constants of the crystal lattice are (a=b 3.25 A^0 c=5.206 A^0).

The crystal structure of zinc oxide is similar of the (VI-II) i.e. the hexagonal compact structure as shown in the (Figure 1).

EXPERIMENTAL PROCEDURE

The ZnO: Pb_3O_4 surfaces were prepared according to (Table 2) by the solid-state reaction method. They were accurately weighed in the required proportion and were mixed and ground well using an agate mortar to turn them into very fine Powders. Grinding of the mixture was carried out for 3 hours for all powder samples. The samples were placed in an oven at 700 C^0 for 3 hours in order to obtain the correct crystal structure. (Figure 3, 4)

RESULTS AND DISCUSSIONS

Figure 5, 6 shows: X-ray diffraction patterns for pure Pb_3O_4 powders. The XRD reveals that pure Pb_3O_4 has a quadrangular structure, corresponding to vertices of (002), (112), (310), (202), (312), (402), (332), and (314). The preferred orientation is (002) for pure Pb_3O_4.

We observed the disappearance of these (100), (201), (103), in samples ZnO: Pb_3

The change in peak intensity is mainly due to the replacement of Zn^{+2} ions by pb^{+4} ions in the ZnO lattice. This process leads to the movement of Zn^{+2} ions in interstitial sites; in fact, that ionic radius of Zn^{+2} iron equals (0.088 nm) is smaller than the ionic radius of pb^{+4} (0.0915 nm).

The relative intensities of undoped and Sb doped powders are calculated.

The distance between crystalline planes values (d) are

Table 1: Same Physical and Chemical Properties of Zinc Oxide [3].

Color	The Shape	Boiling Point (C0)	Melting Point (C0)	Density (g/cm3)	Molar Mass (g/mol)	Crystal Structure
White	Solid	2360	1970	5.67	81.37	Hexa

Figure 1 The compact crystal structure of zinc oxide films.

Table 2: Shows the proportions of the prepared samples.

Parcent wt %	Pb_3O_4	ZnO	The sample
100	0	1	1
80	0.2	0.8	2
50	0.5	0.5	3
20	0.8	0.2	4
0	1	0	5

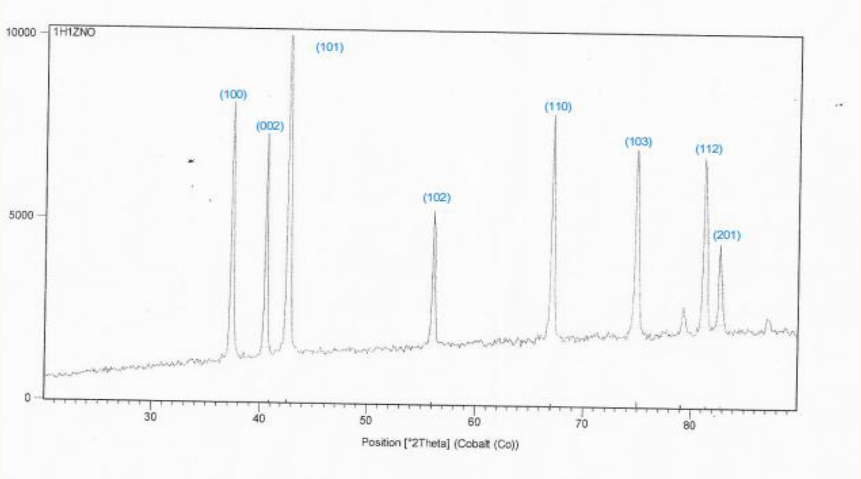

Figure 2 XRD spectra of sample No.1.

calculated by using following relation:

$$2d.\sin\theta = n\lambda \quad (1)$$

Where d is distance between crystalline planes (A), θ is the Bragg angle, λ is the wavelength of X-rays (λ=1.54056 Å).

The crystallite size is calculated from Scherer's equation [4]:

$$D = \frac{0.94\lambda}{\beta \cos\theta} \quad (2)$$

where, D is the crystallite size, λ is the wavelength of X-ray, β is full width at half maximum (FWHM) intensity in radians and θ is Braggs's angle.

The dislocation density is defined as the length of dislocation lines per unit volume and calculated by following equation [5]:

$$\delta = \frac{1}{n^2} \quad (3)$$

The lattice constants a and c for tetragonal phase structure is determined by the relation [6]:

$$\frac{1}{d^2} = \frac{h^2 + k^2}{a^2} + \frac{l^2}{c^2} \quad (4)$$

where d and (hkl) are distance between crystalline planes and Miller indices, respectively.

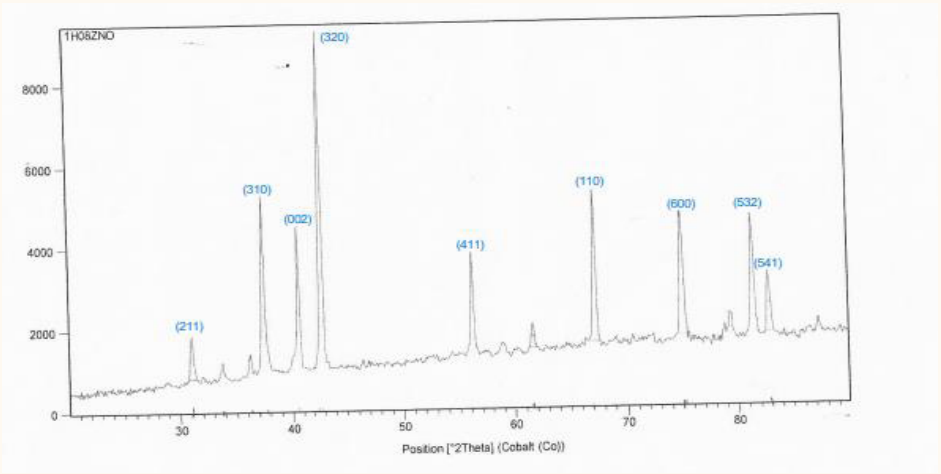

Figure 3 XRD spectra of sample No. 2.

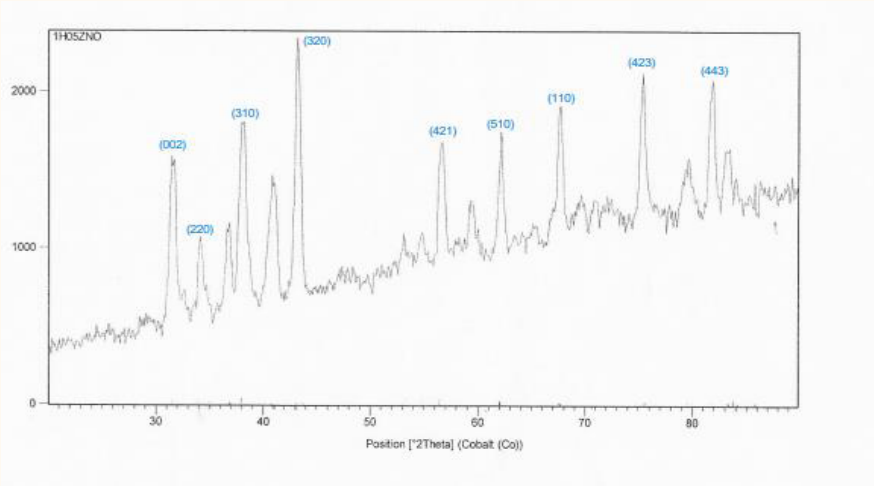

Figure 4 XRD spectra of sample No.3.

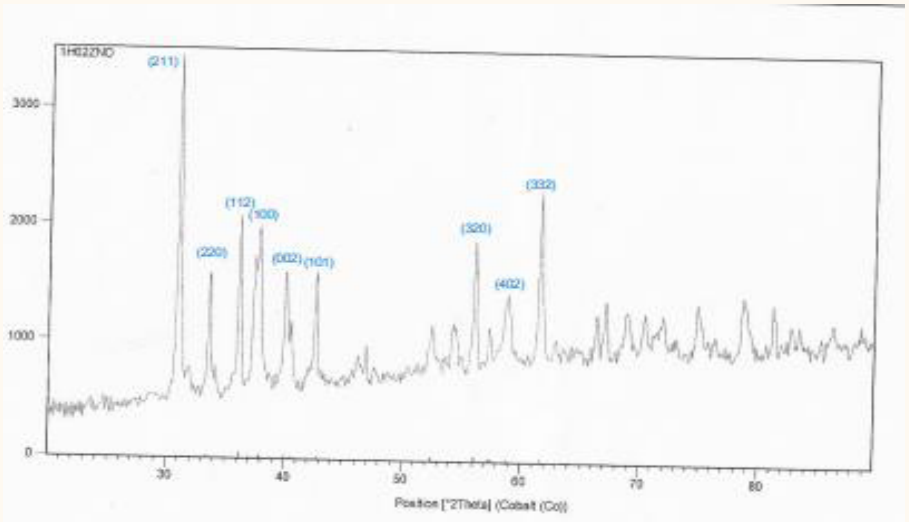

Figure 5 XRD spectra of sample No.4.

The calculated lattice constants a, c values are given in (Table 3, 4). It was seen that a, c and c/a match well with JCPDS data (a=b= 4.737 Å and c= 3.185 Å). The change in peak intensities is basically due to the replacement of Zn^{+2} ions with Pb_3O_4 ions in the lattice of the ZnO.

We notice from (Figure 7) that the sample Pb_3O_4 ZnO shown in (Figure 2) is the best samples compared to the other samples because the average crystal size is larger and the intensity of dislocations is lower in the crystal lattice.

CONCLUSION

This paper presented a study of the structural properties

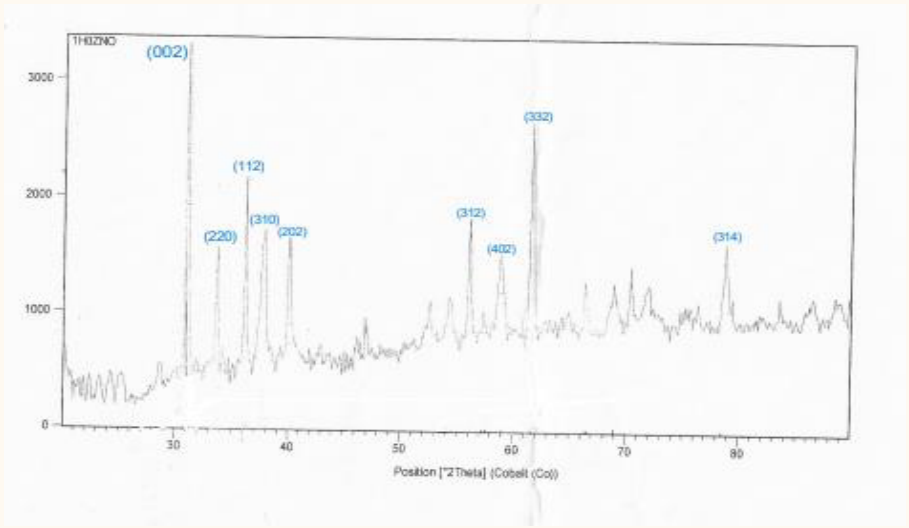

Figure 6 XRD spectra of sample No.5.

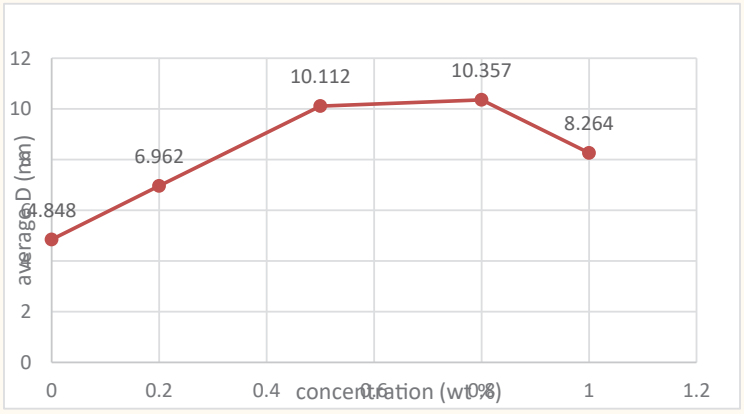

Figure 7 Represents variation of the average grain size with different concentrations of Pb_3O_4 doped ZnO powders.

Table 3: XRD results for sample No.1 form table (2) where θ Bragg angle, D crystal size, d crystal distance, δ dislocation density and int, Miller's integers (hkl) and β width of each pit, a and c are crystal lattice constants.

samples	2θ (deg)	Int	(hkl)	β (deg)	d (Å)	D (nm)	$\overline{D}$ (nm)	$\delta = 10^{+15}\ X\ line/m^2$	$\delta = 10^{+15}\ X\ line/m^2$	Lattic conste	
										AA^0	CA^0
Pb_3O_4 Pure	30	100	-2	0.4	3.456	4.352	5.059	52.798	42.207	8.855	**6.912**

	33.2	47	-220	0.3	3.131	5.849		29.23			
	35.9	65	-112	0.3	2.902	5.892		28.805			
	37.3	52	-310	0.4	2.797	4.437		50.795			
	40.2	49	-202	0.4	2.603	4.476		49.913			
	55.9	56	-213	0.3	1.908	6.346		24.831			
	58.8	46	-402	0.5	1.828	3.86		67.711			
	61.4	81	-332	0.4	1.752	4.889		41.836			
	78.5	49	-314	0.4	1.414	5.428		33.94			

Table 4: XRD results for sample No.2 form table (2) where θ Bragg angle, D crystal size, d crystal distance, δ dislocation density and int, Miller's integers (hkl) and β width of each pit, a and c are crystal lattice constants.

Samples	2θ (deg)	Int	(hkl)	β (deg)	d (Å)	D (nm)	β (nm)	$\delta = 10^{+15} X\ line/m^2$	$\delta = 10^{+15} X\ line/m^2$	Lattic conste	
										AA^0	CA^0
ZnO:Pb_3O_4 80%w	30.9	100	-2	0.35	3.354	4.986	5.655	40.225	40.376	8.779	6.714
	33.5	47	-220	0.25	3.104	7.025		20.263			
	36.2	61	-112	0.25	2.879	7.077		19.966			
	38	58	-100	0.4	2.747	4.446		50.589			
	40.2	46	-2	0.25	2.603	7.163		19.489			
	42.9	46	-101	0.25	2.446	7.227		19.146			
	56.1	55	-320	0.5	1.902	3.811		68.852			
	58.9	42	-421	0.6	1.819	3.219		96.506			
	61.8	67	-332	0.33	1.742	5.939		28.351			
ZnO:Pb_3O_4 20%w	31.1	20	-2	0.33	3.336	5.288	6.504	35.761	26.453	8.876	**6.672**
	37.2	57	-310	0.3	2.804	5.914		28.591			
	40.3	44	-2	0.2	2.596	8.956		12.467			
	42.6	100	-320	0.25	2.462	7.229		19.135			
	57.2	42	-411	0.4	2.033	4.681		45.637			
	67.3	56	-110	0.25	1.614	8.081		15.313			
	75	51	-600	0.35	1.469	6.056		27.266			
	81.3	49	-532	0.33	1.373	6.716		22.171			
	83	35	-541	0.4	1.349	5.613		31.74			

of ZnO and Pb_3O_4 compounds: prepared by solid state reaction method [7]. The X-ray diffraction patterns of the pure zinc oxide sample confirm that it is of poly crystalline nature and hexagonal compact structure and shows the presence of trends (110), (101), (002) and (101) [8]. The preferred orientation is (101), but for ZnO sample similar to Pb_3O_4 by (50-80) % wt.

The preferred trend changes to the (320), and we observed the disappearance of these trends (100), (201), (103) in the ZnO: Pb_3O_4[9-14].

The average crystal size is within the range (4.848-8.264 nm) for all samples. It was determined that the lattice constants c and a for all samples, were the ratio remained constant with the increase of the dopant concentration Pb_3O_4.

REFERENCES

1. Schropp R, Madan A. Properties of Conductive ZnO films for transparent electrodes applications prepared by rf magnetron sputtering. J Appl Phys. 1989; 66: 2027.
2. Hartnagel HL, Dawar AL, Jain AK, Jagadish C. Semiconducting Transparent Thin Films. Institute of Physics Publishing. 1995.
3. Weast RC. Astle MJ. Hand Book of Chemistry and Physics. CRC Press. 1979.

4. Mariappan R, Ponnuswamy V, Suresh P. Effect Of Doping Concentration On The Structural And Optical Properties Of Pure And Tin Doped Zinc Oxide Thin Films By Nebulizer Spray Pyrolysis (NSP) Technique. Super lattices and Microstructures. 2012; 52: 500-513.

5. Turgut G, Keskenler EF, Aydin S, Sonmez E, Dogan S, Duzgun Bet al. Effect Of Nb Doping On Structural, Electrical And Optical Properties Of Spray Deposited SnO2 Thin Films. Super lattices and Microstructures. 2013; 56: 107-116.

6. Gurakar S, Serin T, Serin N. Electrical And Microstructural Properties Of (Cu, Al, In)-Doped SnO2 Films Deposited By Spray Pyrolysis. Advanced Materials Letters. 2014; 5: 309-314.

7. Stanimirova TJ, Atanasov PA, Dimitrov IG, Dikovska AO. Investigation on the structural and optical properties of tin oxide films grown by pulsed laser deposition. J. Optoelectron. Adv. Mater. 2005; 7: 1335-1340.

8. Cetinorgu E, Goldsmith S, Boxman RL. The effect of substrate temperature on filtered vacuum arcdep - osited zinc oxide and tin oxide thin films. Journal of Crystal Growth. 2007; 299: 259-267.

9. Zhai HJ, Wang LS. Probing the Electronic Structure and Band Gap Evolution of Titanium Oxide Clusters (TiO2) (n = 1–10) Using Photoelectron Spectroscopy. J. Am. Chem. Soc. 2007; 129: 3022-3026.

10. Rahal A. Elaboration des verres conducteurs par déposition de ZnO sur des verres ordinaires. Memoire de Magiter. UNIVERSITE D ELOUED. 2013.

11. Thomson D. The Materials and Techniques of Medieval Painting; Courier Corporation: Chicago, IL, USA, 1956.

12. Sharon M, Kumar S, Sathe NP, Jawalekar SR. Study of a Rechargeable Solar Battery with n-Pb3O4 Electrodes. Sol. Cells 1984; 12: 353-361.

13. Zhou Y, Long J, Gu Q, Lin H, Lin H, Wang X. Photoinduced Reactions between Pb3O4 and Organic Dyes in Aqueous Solution under Visible Light. Inorg Chem. 2012; 51: 12594 -12596.

14. Sharon M, Kumar S, Jawalekar SR. Characterization of Pb3O4 films by electrochemical techniques. Bulletin of Materials Science. 1986; 8: 415 - 418.